Journal of Applied Mechanics and Technical Physics, Vol. 49, No. 6, pp. 1040–1046, 2008

ANALYSIS OF THE DYNAMIC RADIAL COMPACTION OF GRANULAR MEDIA

G. Sh. Boltachev and N. B. Volkov

UDC 539.374

The previously developed continual approximation is used to analyze the radial axisymmetric compaction of a granular medium in the presence of a rigid undeformable rod on the symmetry axis. It is shown that, during pulsed loading, high densities close to those corresponding to the nonporous state can be attained due to inertia effects. The influence of the initial radial dimensions of the rod–powder–medium system on the compaction process is analyzed. The problem is found to be scale invariant under various constraints imposed on the ratio of the characteristic dimensions.

Key words: *granular materials, pulsed compaction, inertia effect.*

Introduction. This paper is a continuation of studies [1, 2], devoted to a semi-empirical description of the compaction of a granular medium, in particular, nanopowders based on aluminum oxide [3–5]. The compaction of a granular medium is considered in the continual approximation of a plastically hardened porous solid [6–9]. The characteristics of the AM and α-AM nanopowders studied, experimental compression adiabats, and empirically constructed hardening functions are given in [1, 5]. The latter were used to formulate a closed system of rheological equations and to perform a quasistatic analysis of the radial axisymmetric compaction of nanopowders [1] performed in magnetic-pulsed compaction experiments [3–5]. In [2], a model was constructed that takes into account the effect exerted on the compaction dynamics by the inertial properties of the powder–shell system, which play a decisive role in fast magnetic-pulsed compaction. For the radial compaction of a granular medium in the presence of a rigid rod of radius r_m on the symmetry axis, the following differential equation was obtained to describe the dynamics of the powder–medium interface $[R = R(t)]$ subjected to external magnetic pressure $p_c(t)$:

$$a_0 RA = -\frac{2}{\rho}\frac{\Delta p}{C} - \frac{v_0^2 r_m^2 R^2 B}{(R^2 - r_m^2)^2} - \frac{v_0^2}{C}\frac{\rho_c}{\rho}\Big[2\ln\Big(\frac{R_c}{R}\Big) - 1 + \frac{R^2}{R_c^2}\Big],$$

$$A = 1 - \frac{r_m^2 D}{R^2 - r_m^2} + \frac{\rho_c}{\rho}\frac{2\ln(R_c/R)}{C}, \qquad \Delta p = p_c - p_{c,el} - p_{el}, \tag{1}$$

$$B = \frac{6\Psi + \varphi}{3\varphi}\Big[CD - 2\ln\Big(\frac{R}{r_m}\Big)\Big] - 1 + \frac{r_m^2}{R^2},$$

$$C = \frac{6\Psi + \varphi + 3\varphi r_m^2/R^2}{6\Psi + \varphi}, \qquad D = \frac{6\Psi + 4\varphi}{6\Psi + \varphi}\ln\Big(\frac{(6\Psi + \varphi)R^2 + 3\varphi r_m^2}{(6\Psi + 4\varphi)r_m^2}\Big).$$

Here Ψ and φ are known functions of porosity θ [1]:

$$\Psi(\theta) = \frac{2}{3}\frac{1 - \theta + \theta^2/2}{\theta}\varphi(\theta), \qquad \varphi(\theta) = (1 - \theta)^{5/3}, \tag{2}$$

$a_0 = d^2R/dt^2$ is the acceleration, $v_0 = dR/dt$ is the velocity of the interface of the powder–shell system, $\rho = \rho_{max}(1 - \theta)$ is the density of the granular medium, $\rho_{max} = 3.66$ g/cm^3 for AM powder and $\rho_{max} = 3.986$ g/cm^3

Institute of Electrophysics, Ural Division, Russian Academy of Sciences, Ekaterinburg 620016; grey@iep.uran.ru; nbv@ami.uran.ru. Translated from Prikladnaya Mekhanika i Tekhnicheskaya Fizika, Vol. 49, No. 6, pp. 181–189, November–December, 2008. Original article submitted August 9, 2007.

for α-AM powder, $\rho_c = 8960$ kg/m^3 is the density of the copper shell, $p_{c,el}$ is the part of the external pressure compensated by elastic stresses in copper [2]:

$$p_{c,el} = \Big(1 - \frac{R^2}{R_c^2}\Big)\frac{10K}{\sqrt{3}}\sqrt{\varepsilon_0 + \frac{2}{\sqrt{3}}\ln\Big(\frac{R_0}{R}\Big)}, \tag{3}$$

$\varepsilon_0 = 0.01$, $K = 54.15$ MPa, R_c is the outer radius of the copper shell, R_0 is the initial value R, and p_{el} are the pressure compensated by elastic stresses in the powder [1, 2]:

$$p_{el} = \sqrt{\frac{1-\theta}{2}}\,\frac{(2\Psi + \varphi/3)R^2 + \varphi r_m^2}{\sqrt{(2\Psi + \varphi/3)R^4 + \varphi r_m^4}}\,\tau_0(\Gamma_0). \tag{4}$$

The measure of the accumulated shape change strains Γ_0 that is the argument of the hardening function $\tau_0(\Gamma_0)$ of the nanopowders studied is given by the expression

$$\Gamma_0 = \int\limits_{\theta}^{\theta_0} \sqrt{\Psi + \frac{\varphi}{6}\Big(1 + 3\,\frac{r_m^4}{R^4}\Big)}\;\frac{d\theta}{(1-\theta)^{3/2}}. \tag{5}$$

The dynamics equation (1) is derived under the assumption that the copper shell is incompressible and the granular medium is compacted uniformly:

$$R_c = \sqrt{R_{c,0}^2 + R^2 - R_0^2}, \qquad R = \sqrt{r_m^2 + (R_0^2 - r_m^2)\,\frac{1-\theta_0}{1-\theta}}. \tag{6}$$

Here the subscript 0 denotes the quantities corresponding to the initial state at the time $t = 0$. As shown in [2], the results of numerical solution of the differential equation (1) are in good agreement with experimental data on the density of compacts produced by radial magnetic-pulsed compaction, which confirms that the above assumptions, in particular, the uniform compaction model, are realistic.

In the present study, the developed approach is used to analyze the main regularities of the dynamic compaction of granular media.

We elucidate whether the medium being compacted can reach nearly nonporous states ($\theta = 0$) and study the influence of the radial dimensions of the rod–powder–shell system on the compaction process.

1. Low Porosity Limit. The pressure

$$p_{el} \simeq \Psi^{1/2}\tau_{0,\max} \simeq \sqrt{2/3}\,\tau_{0,\max}/\theta^{1/2} \tag{7}$$

tends to infinity as $\theta \to 0$. Nevertheless, the differential equation (1) admits solutions corresponding to the nonporous state. Indeed, as $\theta \to 0$, Eq. (1) reduces to the equation

$$\alpha\ddot{R} + \beta\dot{R}^2 = \gamma(R - R_{\min})^{-1/2}, \tag{8}$$

where $R_{\min} = (r_m^2 + (R_0^2 - r_m^2)(1-\theta_0))^{1/2}$ is the minimum possible radius R that corresponds to zero porosity,

$$\alpha = R_{\min}\Big[1 - \frac{2r_m^2}{R_{\min}^2 - r_m^2}\,\ln\Big(\frac{R_{\min}}{r_m}\Big) + \frac{2\rho_c}{\rho_{\max}}\,\ln\Big(\frac{R_{c,\min}}{R_{\min}}\Big)\Big] > 0,$$

$$\beta = \frac{\rho_c}{\rho_{\max}}\Big[\frac{R_{\min}^2}{R_{c,\min}^2} - 1 + 2\ln\Big(\frac{R_{c,\min}}{R_{\min}}\Big)\Big] - \frac{r_m^2}{R_{\min}^2 - r_m^2}, \quad \gamma = \frac{2\tau_{0,\max}R_{\min}^{1/2}}{\sqrt{3}\,\rho_{\max}}\sqrt{1 - \frac{r_m^2}{R_{\min}^2}} > 0.$$

Zero porosity is approached at the stage of deceleration of motion ($\dot{R} < 0$ and $\ddot{R} > 0$), which makes it possible to assume that the sign indefinite (but finite) second term on the left side of (8) is negligibly small compared to the other divergent terms of the equation. Then, for the corresponding redefinition $R = R_{\min} + (\gamma/\alpha)^{2/3}y$, we obtain the differential equation

$$\ddot{y}\,\sqrt{y} = 1 \tag{9}$$

with the initial conditions $y(0) = y_0 > 0$ and $\dot{y}(0) = \dot{y}_0 < 0$. Solution (9) is written as

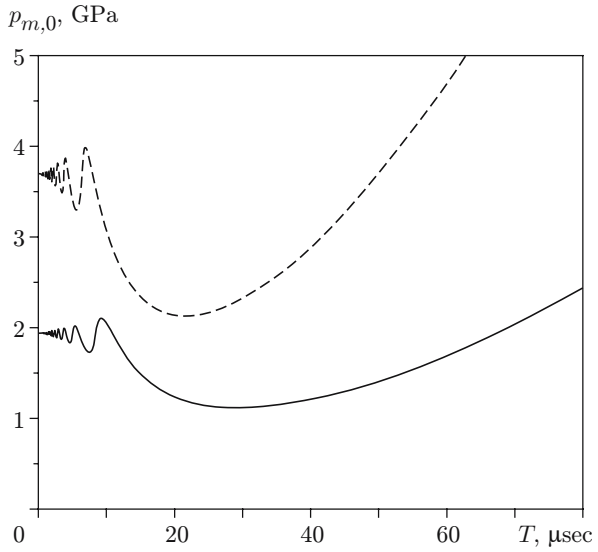

Fig. 1

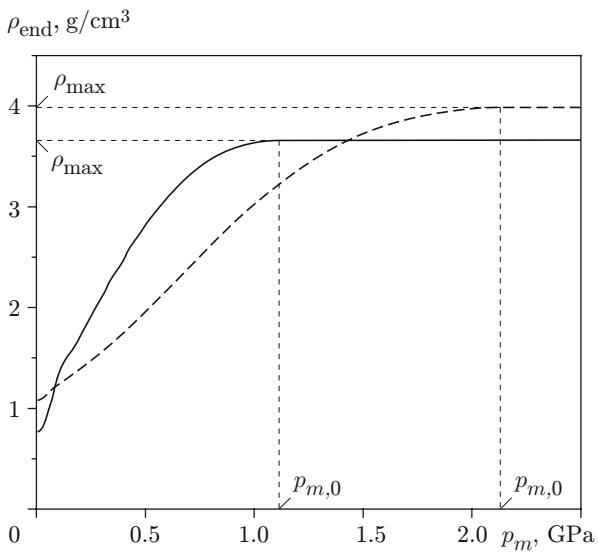

Fig. 2

Fig. 1. External pressure pulse amplitudes (11) beginning at which the nonporous states of AM nanopowder (solid curve) and α-AM nanopowder (dashed curve) are reached ($r_m = 1$ mm, $R_0 = 10$ mm, and $R_{\text{c},0} = 11$ mm).

Fig. 2. End density of compact versus external pressure amplitude: the solid curve refers to AM nanopowder ($T = 29$ μsec); the dashed curve refers to α-AM ($T = 21$ μsec).

$$\dot{y} = -\sqrt{4(\sqrt{y} - \sqrt{y_0}\,) + \dot{y}_0^2}, \tag{10}$$

$$6t = (\dot{y}_0^2 - 4\sqrt{y_0} - 2\sqrt{y}\,)\sqrt{4(\sqrt{y} - \sqrt{y_0}\,) + \dot{y}_0^2} + \dot{y}_0(\dot{y}_0^2 - 6\sqrt{y_0}\,).$$

In the case of rather slow motion where $|\dot{y}_0| < 2y_0^{1/4}$, solution (10) does not reach the value $y = 0$ [for $y = (\sqrt{y_0} - \dot{y}_0^2/4)^2$, the velocity $\dot{y}$ vanishes]. For $\dot{y}_0 = -2y_0^{1/4}$, solution (10) vanishes ($y = 0$ and $R = R_{\min}$), and $\dot{y} = 0$, i.e., the nonporous state is reached without elastic impact. Finally, in the case of great acceleration ($\dot{y}_0 < -2y_0^{1/4}$), the solution reaches the limit $y = 0$ with the nonzero value $\dot{y} = -\sqrt{\dot{y}_0^2 - 4\sqrt{y_0}}$. This corresponds to the elastic impact at the end of compaction with the subsequent reflection, which can result in a fracture of the compact.

Figure 1 gives the amplitudes $p_m = p_{m,0}$ of the sinusoidal external pressure pulse

$$p_{\text{c}} = p_m \sin^2(\pi t/T) \tag{11}$$

beginning at which the nonporous states of AM and α-AM nanopowders are reached in the model analyzed. The characteristics of the AM and α-AM powders are given in [1]. At $p_m < p_{m,0}$, i.e., in the region below the corresponding curve $p_{m,0}(T)$, the compaction process comes to the end at $\theta > 0$ (Fig. 2). At $p_m > p_{m,0}$, an elastic impact is inevitable at the end of the compaction process. The curve $p_m = p_{m,0}$ corresponds to the attainment of the nonporous states without elastic impact. In the quasistatic process, ($T \to \infty$) $p_{\text{el}} \to \infty$ [see (7)]; therefore, the nonporous state is unattainable [8], which leads to an unbounded increase in the amplitude $p_{m,0}$ as $T \to \infty$. The absolute minimum in the curve of $p_{m,0}(T)$ corresponds to the most effective use of the inertial properties of the powder–shell system, and for AM powder, it is reached at $T \simeq 29$ μsec and $p_{m,0} \simeq 1.11$ GPa. Further decrease in the period of the signal T leads to the occurrence of a number of local extrema due to the periodicity of the signal (11). As $T \to 0$, the quantity $p_{m,0}$ tends to a finite value of 1.94 GPa (AM powder), which is equivalent to instantaneous switching-on of an external pressure of halved amplitude ($\simeq$0.97 GPa). The lower compactability of α-AM powder leads to a shift of the curve of $p_{m,0}(T)$ toward higher pressures and higher-frequency signals (the coordinates of the absolute minimum are $T \simeq 21$ μsec and $p_{m,0} \simeq 2.13$ GPa).

Previously, the question of the attainment of the nonporous states due to the dynamics of the compaction process was discussed in [8]. It is noted that this is possible only for the model of a rigid-plastic medium being compacted. Accounting for elastic displacements, strictly speaking, rules out this possibility. However, because the bulk elastic deformation amplitude of crystalline (or polycrystalline) solids is small, the influence of these deformations should apparently be significant only for states whose porosity is less than 1%.

2. Scale Regularities of Compaction. The numerical estimates given above correspond to the following dimensions of the rod–powder–shell system: $r_m = 1$ mm, $R_0 = 10$ mm, and $R_c = 11$ mm. The given values are close to the corresponding parameters in experiments on magnetic-dynamic compaction of nanopowders [1, 2, 5]. Changes in the radius of the rigid rod r_m and (or) thickness of the powder layer R_0 and the copper shell R_c will lead to quantitative, if not qualitative, changes in the results obtained. Let us analyze the nature of these changes.

We consider a proportional change in the geometrical dimensions of the system under which the ratios r_m/R_0 and R_c/R_0 remain constant. We determine the effect exerted by changes in the dimension of the system (which is taken to be the quantity R_0) on the compaction process. It is easy to see that conversion to the normalized variables

$$x = \frac{R}{R_0}, \quad x_c = \frac{R_c}{R_0}, \quad x_m = \frac{r_m}{R_0}, \quad \tau = \frac{t}{R_0}\sqrt{\frac{K}{\rho_{\max}}}$$

eliminates the absolute dimensions of the system, i.e., the quantity R_0, from Eqs. (1)–(6). This implies that the compaction dynamics is described by the universal (independent of the absolute dimensions) relation $\theta(\tau) = \theta(\tau, p_c(\tau), x_m, x_c)$. Thus, a change in all dimensions of the system by a factor of k only leads to a similar scaling of time. For example, the compaction curve presented in Fig. 2 $\rho_{end}(p_m)$ remain constant as the dimensions of the system and the periods T increase by the same factor.

The relative change in the dimensions r_m, R_0, and R_c has a more complex influence on the compaction process. Let us first analyze how compaction is influenced by changes in the radius of the internal rigid rod r_m for constant values of R_0 and R_c. Passage to the limit as $r_m \to 0$ corresponds to the compaction of the continuous cylinder. Thus, expressions (1)–(6) are much simplified. In particular, Eq. (1) describing the motion of the powder–shell interface becomes

$$a_0 R\Big[\frac{\rho}{2} + \rho_c \ln\Big(\frac{R_c}{R}\Big)\Big] = -\Delta p - \frac{\rho_c}{2} v_0^2 \Big[2\ln\Big(\frac{R_c}{R}\Big) - 1 + \frac{R^2}{R_c^2}\Big]. \tag{12}$$

For $r_m \to R_0$, we have the uniaxial compaction problem [1]. In this case, it is convenient to convert to the variable $x = h/h_0 = (R - r_m)/(R_0 - r_m)$, and $h < h_0 \ll r_m$. Then, Eq. (6) becomes

$$x = (1 - \theta_0)/(1 - \theta),$$

and the measure of the accumulated deformations and the limit of the elastically compensated pressure are given by the expressions

$$\Gamma_0 = \int_{\theta}^{\theta_0} \sqrt{\Psi + \frac{2}{3}\varphi}\, \frac{d\theta}{(1-\theta)^{3/2}}, \qquad p_{el} = \tau_0 \sqrt{\Big(\Psi + \frac{2}{3}\varphi\Big)(1-\theta)},$$

which coincide with the corresponding relations of [1]. For $h_0 \to 0$, Eq. (1) reduces to the equation

$$\rho_c R_0 \ln\Big(\frac{R_c}{R_0}\Big) h_0 \Big(\frac{d^2 x}{dt^2}\Big) = -\Delta p. \tag{13}$$

Relation (13) does not contain the density of the medium being compacted ρ because in the limit at $h \to 0$ the influence of the inertial properties of the powder is negligibly small compared to the influence of the inertial properties of the shell being compacted ρ_c.

The transition from compaction of a continuous cylinder [see (12)] to uniaxial compaction of a thin powder layer [see (13)] involves complex dependences of the end density ρ_{end} on the radius of the internal rigid rod (Fig. 3). For small values (curves 1 and 1′) and large values (curves 2 and 2′) of the period T, the dependences $\rho_{end}(r_m)$ differ qualitatively. The cause of these differences becomes clear from an analysis of the dependences $\rho_{end}(T)$ corresponding to various values of r_m.

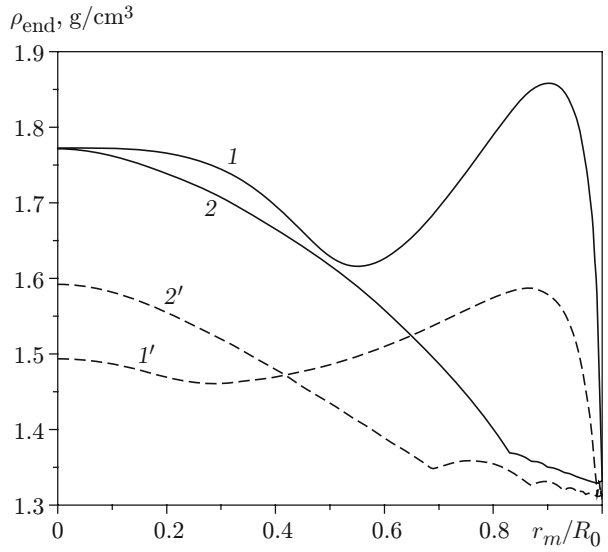

Fig. 3

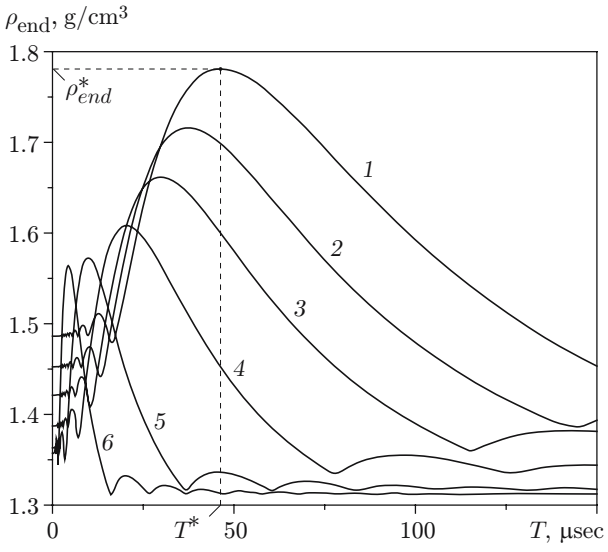

Fig. 4

Fig. 3. End compaction density versus the radius of the internal rigid rod at $R_c/R_0 = 1.1$: the solid curves refer to AM powder ($p_m = 0.2$ GPa) for $T = 20$ (1) and 200 μsec (2); the dashed curves refer to α-AM powder ($p_m = 0.3$ GPa) for $T = 15$ (1′) and 100 μsec (2′).

Fig. 4. End compaction density versus the period T of the external pressure pulse (11) for α-AM nanopowder ($p_m = 0.3$ GPa and $R_c/R_0 = 1.1$) for $r_m/R_0 = 0$ (1), 0.4 (2), 0.6 (3), 0.8 (4), 0.95 (5), and 0.99 (6).

Figure 4 shows a curve of $\rho_{\text{end}}(T)$ for α-AM powder. It is evident that, for the given compaction pressure amplitude p_m, the highest possible density ρ^*_{end} is attained in the absence of a rigid rod (curve 1) at $T = T^*$. The occurrence of a rigid rod on the axis of the system and an increase in its radial dimension r_m leads to a decrease in the absolute maximum of the dependence $\rho_{\text{end}}(T)$ and to a shift in the corresponding curve toward smaller values of T and ρ_{end}. As $h_0 \to 0$, the maximum ceases to decrease and the curves $\rho_{\text{end}}(T)$ become similar. Indeed, it is easy to see that, in conversion to the normalized variable $\tau \sim t/\sqrt{h_0}$, the quantity h_0 disappears from relation (13). This implies that the compaction dynamics is described by the universal dependence $\theta(\tau) = \theta(\tau, p_c(\tau), R_c/R_0)$ independent of the thickness of the powder layer. Thus, a change in the thickness by a factor of k only leads to the corresponding [by a factor of $\sqrt{k}$] scaling of time, and, hence, the period T in Fig. 4.

An analysis of Fig. 4 shows that, for $T \geqslant T^*$, an increase in r_m is accompanied by a monotonic decrease in the density ρ_{end} whereas for $T < T^*$ (on the left of the maximum), the dependence $\rho_{\text{end}}(r_m)$ exhibits more complex behavior. The major factor determining the behavior of the function $\rho_{\text{end}}(r_m)$ is first the total decrease in density, which almost completely suppresses the oscillations of the function $\rho_{\text{end}}(T)$ for small values of T due to the periodicity of the external action (11). With further increase in r_m, the absolute maximum of the dependence $\rho_{\text{end}}(T)$ is shifted to the current value of the period. This leads to the occurrence of the same maximum of the function $\rho_{\text{end}}(r_m)$, which is followed by a fast decrease in ρ_{end}. As $r_m/R_0 \to 1$, all dependences $\rho_{\text{end}}(r_m)$ have weak oscillations that correspond to the oscillations of the function $\rho_{\text{end}}(T)$ for large values of the period and are due to the cyclic nature of the process. With a relatively slow increase in the compaction pressure, the medium being compacted undergoes several cycles of acceleration and deceleration. In the last cycle, the state of the compacted powder is generally characterized by a higher pressure than under quasistatic compaction conditions as $T \to \infty$.

From Fig. 3 it follows that, for small values of r_m, the end density depends weakly on the radius of the rigid rod. As $r_m \to 0$, this behavior of the functions $\rho_{\text{end}}(r_m)$ does not depend on the type of nanopowder and the parameters of the compacting pulse (11), which is a consequence of the initial equations (1)–(6) describing the dynamics of the medium being compacted. The expansion of these equations in r_m does not contain linear terms, and the main order terms are followed by terms of type r_m^2 and $r_m^2 \ln(R/r_m)$. This in turn, leads to the vanishing

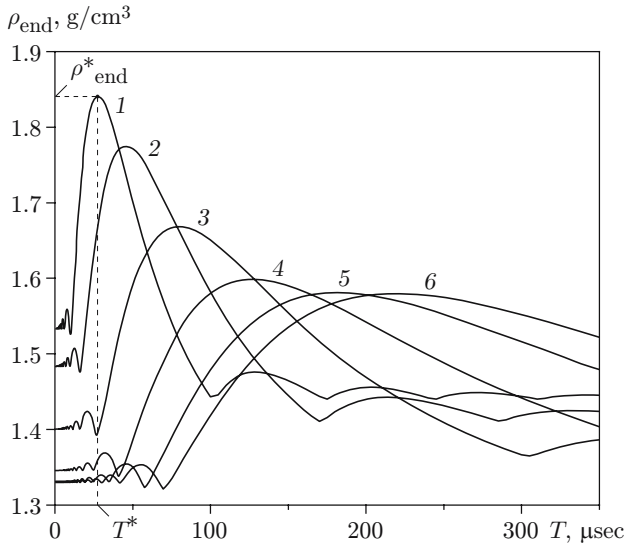

Fig. 5

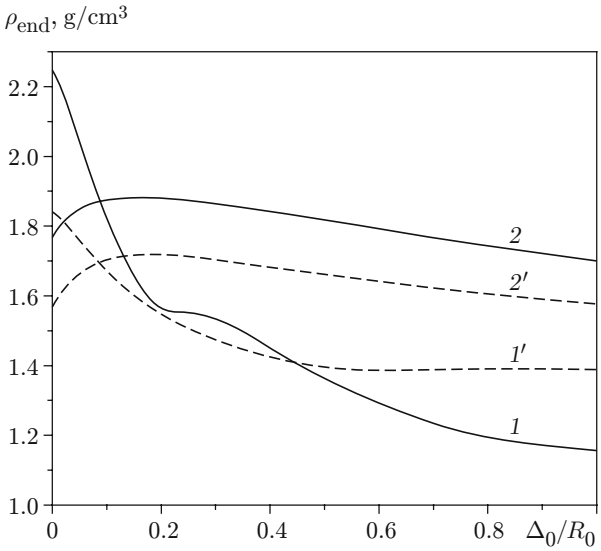

Fig. 6

Fig. 5. End compaction density versus the period T of the external pressure pulse (12) for α-AM nanopowder ($p_m = 0.3$ GPa and $r_m/R_0 = 0.1$): 1) $R_{\text{c},0} = R_0$ (negligibly thin shell); 2) $R_{\text{c},0}/R_0 = 1.1$; 3) $R_{\text{c},0}/R_0 = 1.5$; 4) $R_{\text{c},0}/R_0 = 3$; 5) $R_{\text{c},0}/R_0 = 10$; 6) $R_{\text{c},0}/R_0 = 30$.

Fig. 6. End compaction density versus initial thickness of the external conducting shell at $r_m/R_0 = 0.1$: solid curves refer to AM powder ($p_m = 0.2$ GPa) for $T = 34.4$ (1) and 150 (2) μsec; dashed curves refer to α-AM powder ($p_m = 0.3$ GPa) for $T = 27.6$ μsec (1′) and 70 μsec (2′).

of the first derivative of the function $\rho_{\text{end}}(r_m)$ as $r_m \to 0$, as a result of which the values of ρ_{end} become constant for small values of r_m.

Let us analyze the influence of the initial thickness of the external conducting shell $\Delta_0 = R_{\text{c},0} - R_0$ on the compaction for constant values of R_0 and r_m. For a thin shell ($\Delta_0 \ll R_0$), the governing relations (1), (3), and (6) can be expanded in series in the parameter Δ_0. In particular, from relations (6) and (3), as a first approximation, we obtain

$$\Delta = R_{\text{c}} - R = \Delta_0 R_0/R, \qquad p_{\text{c,el}} = \sqrt{2}\,\tau_{0,\text{c}}\Delta/R$$

($\tau_{0,\text{c}}$ is the yield stress of the shell material), in this case, the equation describing the dynamics of the shell [2], becomes

$$p = p_{\text{c}} - \sqrt{2}\,\tau_{0,\text{c}}\Delta/R + \rho_{\text{c}} a_0 \Delta,$$

where p is the pressure on the inner surface of the shell, i.e., the pressure from the powder being compacted. For $\Delta_0 \to 0$ (or $R_{\text{c}} \equiv R$), the shell is absent. In this case, the pressure on the powder p is equal to the external pressure p_{c}, and the conducting shell is only an instrument for producing magnetic pressure.

As $R_{\text{c}} \to \infty$, the stresses (3) which are elastically compensated by the shell remain finite. Hence, an increase in the thickness of the conducting shell to arbitrarily large values does not rule out the possibility of compaction. Thus, for $R_{\text{c}} \to \infty$, the starting pressure transforming the inner surface of the shell to the plastic state is $p_{\text{c,el}} = K/\sqrt{3} \simeq 31$ MPa. In this case, Eq. (1) reduces to the equation

$$\rho_{\text{c}}(Ra_0 + v_0^2)\ln(R_{\text{c}}/R) = -\Delta p. \tag{14}$$

For large values of R_{c}, we can ignore the dependence $R(t)$ in the argument of the logarithm and set

$$\ln(R_{\text{c}}/R) = \ln(R_{\text{c}}/R_0) + \ln(R_0/R) \simeq \ln(R_{\text{c}}/R_0).$$

Then, converting to the variable $\tau \sim t/(R_0\sqrt{\ln(R_c/R_0)})$ it is possible to eliminate R_c and R_0 from the equation describing the compression dynamics (14). The latter, in particular, implies that the end density is described by the universal (independent of the shell thickness) dependence $\rho_{end} = \rho_{end}(T_r, p_m(\tau), r_m/R_0)$, where $T_r = T(\ln(R_c/R_0))^{-1/2}$, i.e., the curves of $\rho_{end}(T)$ given in Fig. 5 become similar.

The effect of the thickness of the conducting shell on the end density is illustrated in Fig. 6. The maximum compaction is achieved in the limit of an infinitely thin shell (the coordinates of the absolute maximum in curve 1 in Fig. 5 are $T^* \simeq 27.6$ μsec $\rho^*_{end} \simeq 1.841$ g/cm^3 for α-AM powder; accordingly, $T^* \simeq 34.4$ μsec and $\rho^*_{end} \simeq 2.247$ g/cm^3 for AM powder). An increase in the thickness Δ_0 leads to an increase in the value of $p_{c,el}$, which reduces the compaction, and to an increase in the inertial characteristics of the system, which, in turn, shifts (stretches) the dependence $\rho_{end}(T)$ toward larger values of the period T. As a result, for small values of the period ($T \leqslant T^*$), an increase in the thickness of the conducting shell is accompanied by a sharp decrease in the attained density ρ_{end} (see Fig. 6). For $T > T^*$, the character of the dependence $\rho_{end}(\Delta_0)$ changes. The influence of the above factors leads to the occurrence of an insignificant maximum for values $\Delta_0 \simeq 0.2R_0$. We also note that insignificant oscillations in curves 1 and 1′ (see Fig. 6) are a consequence of the periodicity of the signal used (11).

Conclusions. The characteristic features of the dynamic process of radial axisymmetric compaction of granular media in the presence of a rigid rod on the symmetry axis were analyzed using the previously developed continual approximation of a plastically hardening porous solid. The possibility of attaining the nonporous states was shown (ignoring elastic deformations); for the nanopowders studied, the external pressure amplitudes at which the compaction process is inevitably ended with elastic impact were calculated. The equations describing the dynamics of the process were shown to be scale invariant under proportional changes in all radial dimensions of the rod–powder–shell system and similar scaling of time. The influence of a relative change in the dimensions was also analyzed. In particular, it was established that in the limit of a thin rigid rod ($r_m \to 0$), its thickness does not influence the compaction process and, hence, the density of the final compact. The findings open up a possibility of controlling the compaction process for the purpose manufacturing of articles with required parameters.

We thank V. V. Ivanov for attention in the work and useful discussions.

This work was supported by the Russian Foundation for Basic Research (Grant No. 05-08-33387).

REFERENCES

1. G. Sh. Boltachev, N. B. Volkov, S. V. Dobrov, et al., "Modeling the radial magnetic-pulsed compaction of a granular medium in a quasistatic approximation," *Zh. Tekh. Fiz.*, **77**, No. 10, 58–67 (2007).
2. G. Sh. Boltachev, N. B. Volkov, V. V. Ivanov, and S. N. Paranin, "Dynamic compaction model for a granular medium," *J. Appl. Mech. Tech. Phys.*, **49**, No. 2, 336–339 (2008).
3. V. V. Ivanov, S. N. Paranin, A. N. Vikhrev, and A. A. Nozdrin, "Effectiveness of dynamic compaction of nanosize powders," *Materialovedenie*, No. 5, 49–55 (1997).
4. V. V. Ivanov, S. N. Paranin, A. V. Nikonov, et al., "Producing tubes from Al_2O_3 and ZrO_2 ceramics by electrodynamic compaction and ordinary sintering," in: *Problems of Nanocrystalline Materials* [in Russian], Izd. Ural. Otd. Ross. Akad. Nauk, Ekaterinburg (2002), pp. 536–546.
5. S. Paranin, V. Ivanov, A. Nikonov, et al., "Densification of nano-sized alumina powders under radial magnetic pulsed compaction," *Adv. Sci. Technol.*, **45**, 899–904 (2006).
6. I. F. Martynova and M. B. Shtern, "Equation of plasticity of a porous solid with true deformations of the base material taken into account," *Poroshk. Metallurg.*, No. 1, 23–29 (1978).
7. V. V. Skorokhod and L. I. Tuchinskii, "Plasticity condition for porous solids," *Poroshk. Metallurg.*, No. 11, 83–87 (1978).
8. M. B. Shtern, G. G. Serdyuk, L. A. Maksimenko, Yu. V. Trukhan, and Yu. M. Shulyakov, *Phenomenological Theories of Powder Compaction* [in Russian], Naukova Dumka, Kiev (1982).
9. V. V. Skorokhod, *Rheological Bases of Sintering Theory* [in Russian], Naukova Dumka, Kiev (1972).